DOI: 10.1002/ejic.200701312

Structure–Catalytic Activity Relationship in Bridging Silacycloalkyl Ring Conformations of Constrained Geometry Titanium Complexes

Eugene Kang,[a] Sung-Kwan Kim,[a] Tae-Jin Kim,[a] Jae-Ho Chung,[a] Jong Sok Hahn,[b] Jaejung Ko,*[a] Myung-Ahn Ok,[b] Minserk Cheong,[c] and Sang Ook Kang*[a]

Keywords: Si ligands / Cyclopentadienyl ligands / Titanium / Isomers / Structure–activity relationships

A series of cyclic silylene-bridged (amidocyclopentadienyl)-dichlorotitanium(IV) complexes [$TiCl_2${η^5-1-(CySi*t*BuN-κN)-2,3,4,5-R_4-C_5}] was prepared, where CySi = silacyclobutyl (**a**), silacyclopentenyl (**b**), silacyclopentyl (**c**), and silacyclohexyl (**d**); R = H (**4**), Me (**5**). The starting silane, dichlorosilacycloalkane $CySiCl_2$ (**1**), was treated with NaCp ($LiCp^*$), followed by LiNH*t*Bu to yield the cyclic silylene-bridged ligands (R_4C_5)CySi(NH*t*Bu) [R = H (**2**); Me (**3**)]. Subsequent deprotonation with *n*-butyllithium, followed by transmetalation with $TiCl_4$ yielded the desired constrained geometry complexes (CGCs) (CpCySiN*t*Bu)$TiCl_2$ (**4**) and (Cp^*CySiN*t*Bu)$TiCl_2$ (**5**). The structures of the resulting cyclopentadienyl- (**4b** and **4c**) and tetramethylcyclopentadienyl(silacycloalkyl)amidotitanium(IV) dichloride (**5a**, **5c**, and **5d**) species were studied by using X-ray crystallography to obtain geometrical information on cyclic silylene-modified CGCs. The ethylene polymerization by the cyclic silylene-bridged CGCs **4** and **5** was examined to verify the structure–catalytic activity relationship derived from variation of the size of a cyclic silylene ring. Indeed, the size of the cyclic silylene ring at the 1,1′-position of **4** and **5** affected the catalytic activities through the ethylene polymerization. Systematic increase in the catalytic activities was observed as the cyclic silylene-bridging unit was expanded from a four- to six-membered ring. In the present study, we found that CGCs of Ti^{IV} with a six-membered silylene-bridged ligand (**5d**) produced active catalytic species for the formation of polyethylene with $M_w = 42.7 \times 10^{-4}$ g mol^{-1} and $M_w/M_n = 2.1$ with excellent catalytic activities (20.9 kg polymer per mmol of Ti). When titanium(IV) dimethyl complex (**6d**) was applied in continuous polymerization process, impressive high catalytic activity on copolymerization with 1-octene was observed.

Introduction

The concept, "constrained geometry," came from a unique ligand layout designed from the tetrahedral structural motif of a silylene-bridged chelate consisting of two dissimilar coordinating functionalities: η^5-cyclopentadienide and η^1-amide.[1] A wide variety of group 4 metal complexes based on this ligand system has been reported. The group 4 metal systems with silylene-bridged constrained geometry were found to be significantly used in homogeneous Ziegler–Natta catalysis.[2] Especially, the titanium systems were shown to yield excellent ethylene/1-alkene copolymerization catalysts.[3] Many variations were carried out on the η^5-cyclopentadienide and η^1-amide units.[4–7] However, there are much fewer reports on systems related to the variation of the silylene-bridging unit.[8] To this end, we have studied the structure–catalytic activity relationship of cyclic silylene-bridged constrained geometry complexes (CGCs), in which the bridging cyclic silylene unit is varied in ring size from four to six.[9] Six-membered cyclic silylene-bridged CGC **5d** exhibited enhanced catalytic activity as a result of the formation of a stable six-membered ring at the bridging position. Here, we report the full details of the syntheses and characterizations of new types of the cyclic silylene-modified CGCs **4** and **5**. Furthermore, theoretical calculations for this unique series of CGCs were performed to account for the origin of the geometric changes on the silicon atom, as shown in Scheme 1.

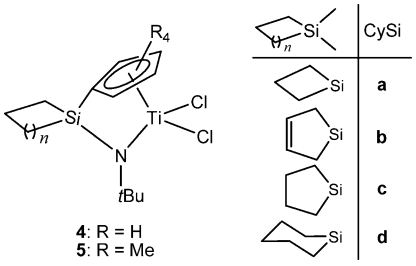

Scheme 1. New types of cyclic silylene-bridged cyclopentadienyl- (**4**) and tetramethylcyclopentadienyl(silacycloalkyl)amido titanium(IV) dichloride (**5**).

[a] Department of Chemistry, Korea University,
208 Seochang, Chochiwon, Chung-nam 339-700, Korea
Fax: +82-41-867-5396
E-mail: sangok@korea.ac.kr
[b] R&D Center, SK Corporation,
140-1 Wonchon-dong, Yuseong-gu, Daejeon 305-712, Korea
[c] Department of Chemistry and Research Institute for Basic Sciences, Kyung Hee University,
Seoul 130-701, Korea
Supporting information for this article is available on the WWW under http://www.eurjic.org or from the author.

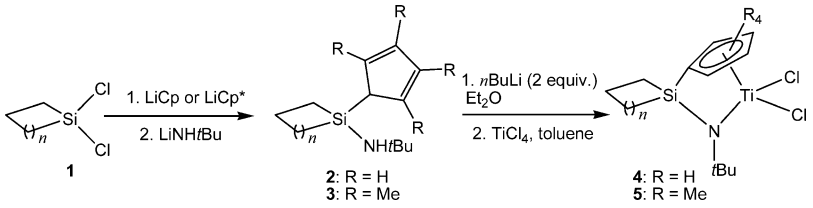

Scheme 2. Preparation of new types of cyclic silylene-bridged cyclopentadienyl- (**4**) and tetramethylcyclopentadienyl(silacycloalkyl)amido titanium(IV) dichloride (**5**).

The titanium(IV) dimethyl complex of **5d**, [$TiMe_2$\{η^5-1-($CyC_5H_{10}SitBuN$-κN)-2,3,4,5-Me_4C_5\}] (**6d**), was produced in reasonable yields by the reaction of **3** with MeLi (4 equiv.), followed by $TiCl_4$. Compound **6d** exhibited higher catalytic activity when copolymerization of ethylene and 1-octene was carried out in a continuous polymerization process.

Results and Discussion

Synthesis and NMR Characterization of Silacycloalkyl-Bridged (Amidocyclopentadienyl)dichlorotitanium(IV) Complexes 4 and 5

Our synthesis routes to (CpCySiN)$TiCl_2$ (**4**) and (Cp*CySiN)$TiCl_2$ (**5**) are shown in Scheme 2. Chelating η^5;η^1-CpN-type ligands with a cyclic silylene bridge are readily accessible by the in situ reaction of lithium amide with cyclopentadienyl- and tetramethylcyclopentadienyl silacycloalkyl chlorides, respectively. Compounds **2** and **3** (colorless liquids) are readily accessible by a procedure similar to the one for the synthesis of the dimethylsilylene-bridged ligand Me_2Si(Cp*)(NH*t*Bu).[10] For example, the reaction of Cp with *n*-butyllithium followed by the addition of $CySiCl_2$ (**1**) gives cyclopentadienylsilacycloalkyl chloride in good yield. Subsequent reaction with lithium amide produces silacycloalkylcyclopentadienyl amide (**2**).

The ligand systems used were multidentate, which have a potential coordination mode of η^5- and η^1-type bondings. The lithium salt was taken as the starting material for the synthesis of the metal amides. The reaction of $TiCl_4$ (3.0 mmol) and the dilithium salt of **2** and **3** (1 equiv.) in toluene led to the formation of [$TiCl_2$\{η^5-1-(CySi*t*BuN-κN)-2,3,4,5-R_4C_5\}] [R = H (**4**), Me (**5**)] in moderate yield (10–21%). Compounds **4** and **5** were purified by low-temperature recrystallization from hexane/pentane, forming yellow crystals. Satisfactory elemental analyses were obtained for **4** and **5** (see Experimental Section) and the ^{1}H and ^{13}C NMR spectroscopic data were consistent in terms of indicating the presence of the cyclopentadienyl silylamide ligand (see Supporting Information).

The ^{1}H NMR signals for the N*t*Bu group in **4** and **5** are at a field lower than that for the free ligand. This can be explained by the presence of a tetrahedral geometry for the amide and evidence of Ti–N coordination in solution. This observation is similar to that found in dimethylsilyl-bridged constrained-geometry-type complexes [$TiCl_2$\{η^5-1-(Me_2Si*t*-BuN-κN)-2,3,4,5-R_4-C_5\}] [R = H (**4**), Me (**5**)].[11]

The data for **4** and **5** also reveal that the replacement of a Cp with a Cp* ring has little effect on the N*t*Bu values in both the ^{1}H and ^{13}C NMR spectra. The ^{1}H NMR spectra of **4** show two multiplets for the α- and β-cyclopentadienyl ring protons in the AA′BB′ system and broad overlapping multiplets for the methylene groups of the silacycloalkyl-bridging unit.[12] The ^{1}H NMR signals for Cp in **4** are downfield of those for the free Cp, which indicates that there is Ti–Cp coordination in solution. The reaction proceeded with low yield but gave preferential formation of the cyclic silylene-bridged CGCs. In the case of tetramethylcyclopentadienyl derivatives **5**, similar downfield shifts of both the N*t*Bu and cyclopentadienylmethyl resonances were observed as an evidence of titanium-atom coordination.[13] As a result of the low yield of the titanium dichloride complexes of **5**, an alternative approach to obtain dimethyltitanium(IV) CGC was sought.[14] In fact, **6d** was prepared in situ by treating **3d** with MeLi (4 equiv.), followed by $TiCl_4$ (Scheme 3).

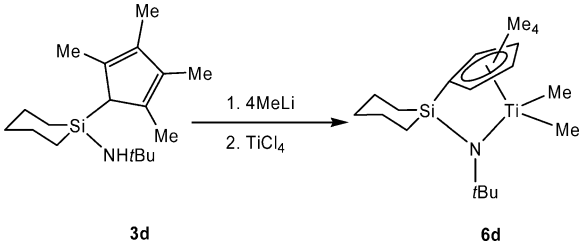

Scheme 3. High yield synthesis of dimethylated constrained-geometry-type complexes; tetramethylcyclopentadienyl(silacyclohexyl)-amido titanium(IV) dimethyl (**6d**).

Structural Features of 4b, 4c, 5a, 5c, and 5d

The molecular structures of the cyclic silylene-bridged complexes of (CpCySiN)$TiCl_2$ (**4b** and **4c**) and (Cp*CySiN)$TiCl_2$ (**5a**, **5c**, and **5d**) were determined by X-ray crystallography. Optimized structures of compounds **4b**, **4c**, **5a**, **5c**, and **5d** are presented in Figures 1, 2, 3, 4, and 5. A comparison of some general structural features is given in Table 1 together with some relevant data of the dimethylsilylene-bridged CGC of (Cp*SiN)$TiCl_2$. Some of the general structural characteristics of the classes of the (CpCySiN)$TiCl_2$ (**4b** and **4c**) and (Cp*CySiN)$TiCl_2$ (**5a**, **5c**, and **5d**) complexes are discussed below.

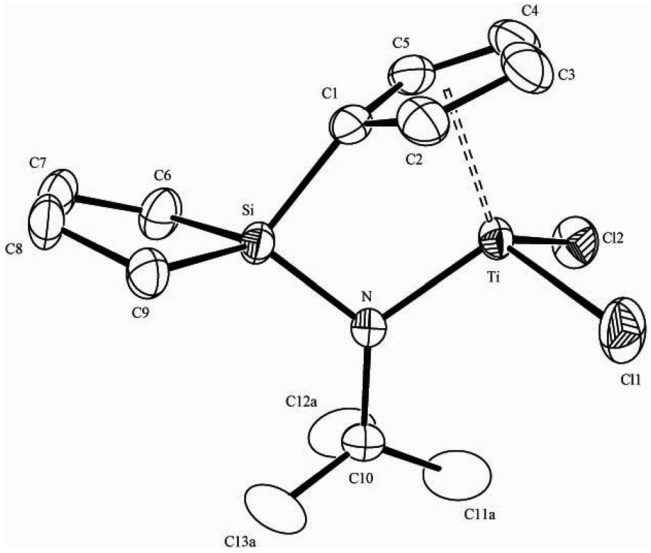

Figure 1. The crystal structure of **4b**. There is some disorder in the *t*Bu groups, which is pronounced at C11/C12/C13. Only C11a, C12a, and C13a are shown in the diagram, with C11b/C12b/C13b omitted. Hydrogen atoms have been omitted for clarity, and the ellipsoids are drawn at the 30% probability level.

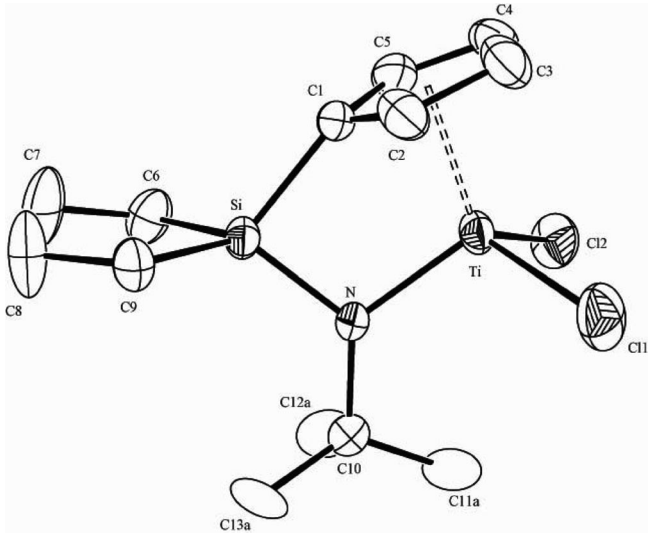

Figure 2. The crystal structure of **4c**. There is some disorder in the *t*Bu groups, which is pronounced at C11/C12/C13. Only C11a, C12a and C13a are shown in the diagram, with C11b/C12b/C13b omitted. Hydrogen atoms have been omitted for clarity, and the ellipsoids are drawn at the 30% probability level.

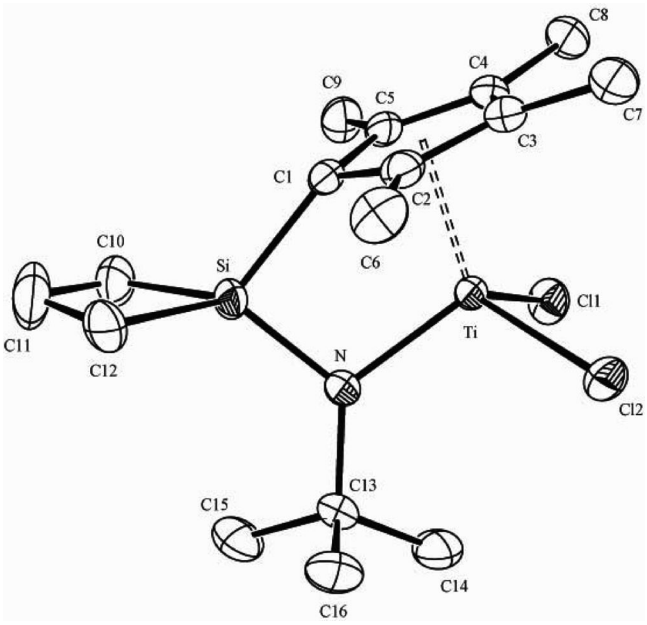

Figure 3. The crystal structure of **5a**. Hydrogen atoms have been omitted for clarity, and the ellipsoids are drawn at the 30% probability level.

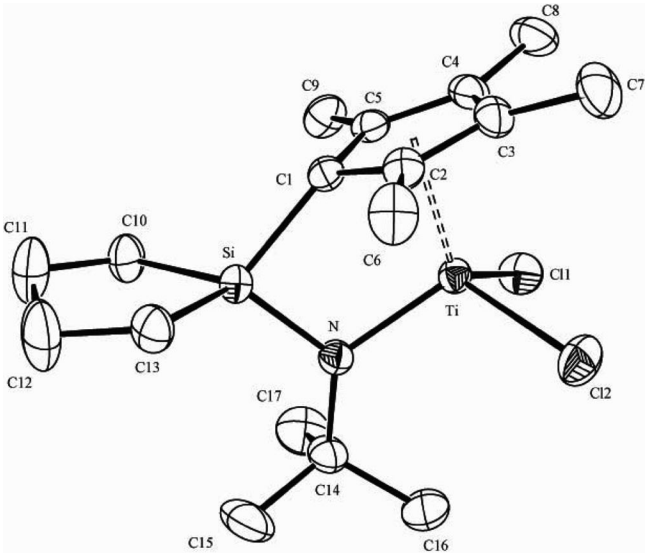

Figure 4. The crystal structure of **5c**. Hydrogen atoms have been omitted for clarity and the ellipsoids are drawn at the 30% probability level.

Overall, bond lengths and angles around the titanium metal center are similar to those found in (Cp*SiN)-$TiCl_2$.[15] The central titanium atom in all of the structures studied is pseudotetrahedrally coordinated to a pair of chloride ligands (Ti–Cl1 2.257/2.275 Å, Ti–Cl2 2.258/2.285 Å), the amido nitrogen, and the Cp/Cp* ligand of the (Cp/Cp*)CySiN ligand system. The Cp* ligand is η^5-coordinated to titanium, but rather unsymmetrically, probably because of the strain imposed on the system by the short C1 bridge. The Ti–C1 linkage (2.268/2.288 Å) is shorter than the Ti–C2/C5 (2.297/2.339 Å) bonds, which in turn are themselves slightly shorter than the Ti–C3/C4 linkages (2.391/2.455 Å) (for each value see Table 1). The connecting C1–Si vector between the Cp ring and the C1 bridge is bent out of the Cp ligand plane toward the metal center. The corresponding Cp(centroid)–C1–Si angle is 150.30/151.53°, which is smaller than that found in (Cp*SiN)$TiCl_2$ (151.18/152.03°). The endocyclic C1–Si–N bond angle is 90.40/91.46°, which is far from that for the tetrahedral sp^3 Si value. The "constrained geometry" character in a series of related compounds is probably best characterized by the

Table 1. Compilation of characteristic structural parameters of **4b**, **4c**, **5a**, **5c**, **5d**.[a].

	4b	**4c**	**5a**	**5c**	**5d**[b]		CGC[c]
M–C1	2.288(3)	2.268(5)	2.2734(19)	2.269(2)	2.273(4)	2.268(4)	
M–C2	2.309(3)	2.297(5)	2.321(2)	2.335(2)	2.339(4)	2.326(4)	
M–C3	2.391(3)	2.394(6)	2.432 (2)	2.433(3)	2.455(4)	2.444(4)	
M–C4	2.407(3)	2.410(6)	2.431(2)	2.440(3)	2.443(4)	2.443(4)	
M–C5	2.329(3)	2.322(6)	2.337(2)	2.328(2)	2.327(4)	2.335(4)	
M–$Cp_{(centr)}$	2.017	2.012	2.025	2.027	2.036	2.031	2.030
M–N	1.9136(19)	1.915(4)	1.9244(16)	1.922(2)	1.929(3)	1.920(3)	1.907(3)
$Cp_{(centr)}$–C1–Si	150.30	151.53	151.18	152.03	151.80	151.79	
N–M–$Cp_{(centr)}$	106.85	107.13	107.44	107.50	108.11	107.96	107.6
C1–Si–N	91.04(11)	90.4(2)	91.24(8)	90.46(10)	91.24(8)	91.0(2)	
Σ N angles	360	360.07	359.75	359.81	359.14	359.32	
Cl1–M–Cl2	103.38(4)	103.50(8)	102.30(2)	102.64(3)	103.43(5)	104.76(5)	102.97(7)
M–Cl1	2.2612(9)	2.2569(17)	2.2717(6)	2.2720(8)	2.2717(6)	2.275(1)	2.264(1)
M–Cl2	2.2634(9)	2.2580(18)	2.2751(6)	2.2759(9)	2.2751(6)	2.285(1)	2.264(1)

[a] Bond lengths in Å, angles in °. [b] Value from two independent molecules in the unit cell. [c] $(C_5Me_4)(C_2H_6)SiNtBuTiCl_2$.

Cp(centroid)–Ti–N angle, which responds sensitively to steric and geometrical changes. In this series it amounts to 106.84/108.10°. The coordination geometry of the ligand nitrogen atom is trigonal planar. Overall, the apparent structural differences are not found in exocyclic silylene-bridged constrained-geometry-type complexes when they are compared with the noncyclic silylene-bridged complex $(Cp^*SiN)TiCl_2$. Because of the formation of silacycloalkyl rings, the bridgehead position of the silicon atom experiences distorted tetrahedral environment, resulting in strained exocyclic bond angles. However, despite the large change in the C–Si–C bond angles of cyclic silylenes on going from 80.13° for **5a** to 100.5° for **5d**, the [C(Cp)–Si–N]- and [Cp(centroid)–Ti–N] internal bond angles remain constant.

Conformational Effects Derived from Exocyclic Ring Formation

The unique feature of cyclic silylene-bridged constrained-geometry-type complexes studied is related to the formation of a cyclic ring around a silicon atom. Depending on the size of the cyclic silylene ring, the exocyclic C–Si–C ring varies: as the size of the ring increases, the corresponding exocyclic bond angle becomes larger.

In fact, when four- to six-membered rings are associated with the CGC system, the angle expands to 100.5°. The increase in the exocyclic bond angles causes a folding of the exocyclic ring and leads to the formation of stable chair conformation. In fact, in the solid structure of **5d**, the Si and C12 atoms are pushed away from the plane defined by the C10, C11, C13, and C14 atoms by 0.67 and 0.91 Å, respectively. Moreover, because of the formation of a stable six-membered exocyclic ring, the Cp* and *t*Bu amido ligands now pose in the least-hindered position of the most-stable conformation. Indeed, in the structure of **5d**, the Cp* ligand takes up the axial position, whereas the amido ligand is positioned in the equatorial position in a stable chair form of a six-membered silacyclohexyl ring. It has been noted that there are four possible conformational isomers associated with this six-membered silacyclohexyl bridging unit, which are illustrated in Scheme 4. Among them, conformational isomer **5d**-c–a was confirmed by the X-ray crystal structural study of **5d**, as shown in Figure 5.

However, in all other bridged silacycloalkyl rings (four- and five-membered rings), conformational isomers would not be possible due to the planarity of the ring. On the basis of the results of the X-ray structural studies, it was observed that the silicon atoms were displaced only a few hundredths of an angstrom from the planes defined

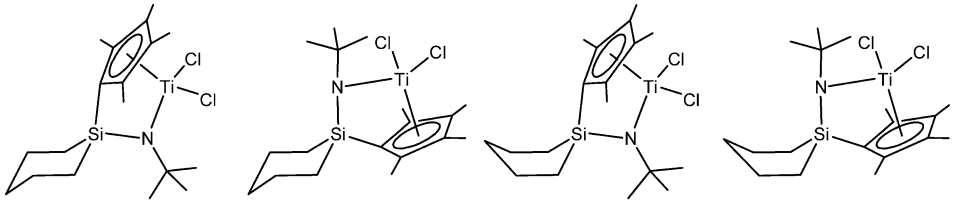

Scheme 4. Possible conformational isomers associated with complex **5d**. The second letter "c" denotes the chair form, whereas "b" denotes the boat form. The third letter "a" and "e" symbolize the position of the Cp* ring in either the axial or equatorial position, respectively.

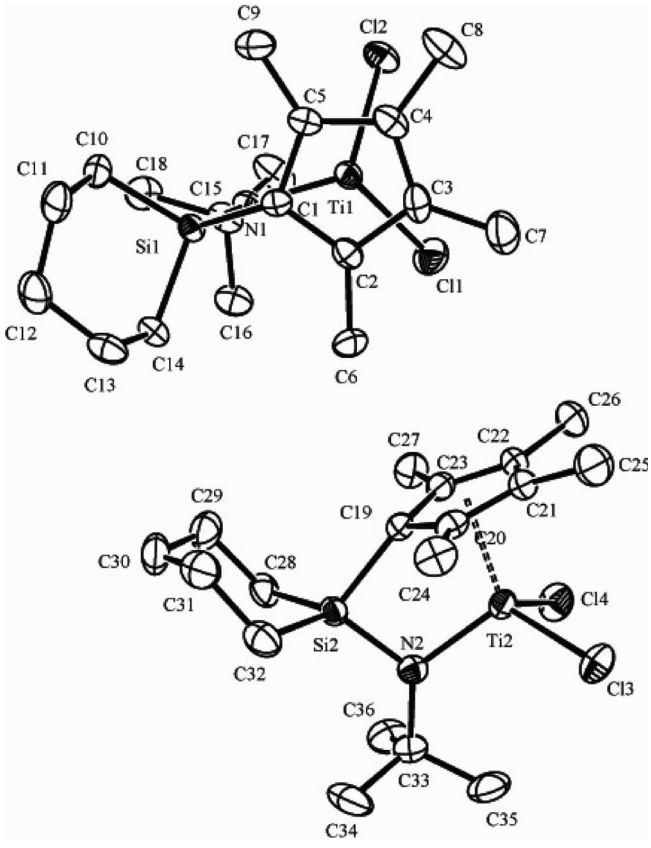

Figure 5. The crystal structure of **5d**. Hydrogen atoms have been omitted for clarity, and the ellipsoids are drawn at the 30% probability level.

by the rest of the carbon atoms of the silacycloalkanes and alkenes: 0.3982(52), 0.1306(109), 0.1761(85), and 0.0193(62) Å for **4b**, **4c**, **5a**, and **5c**, respectively.

Olefin Polymerization Experiments

Representative data of ethylene polymerization reactions of **4** in combination with $Ph_3CB(C_6F_5)_4/Al(iBu)_3$ are listed in Table 2. For direct comparison we carried out ethene polymerization experiments under our condition by using a Si_1-bridged $(Cp^*SiN)TiCl_2$ system.[5,10,16] Complexes **4** appeared to be less-active catalyst systems relative to the reference catalyst $(Cp^*SiN)TiCl_2$ for ethylene polymerization, with activities of 0.22, 0.71, 0.83, 2.45 kgPE mmolTi^{-1}, respectively, for **4a**, **4b**, **4c**, and **4d**. The activity of **4** increased with an increase in the size of the silacycloalkyl bridge and reached a maximum in six-membered cyclic silylene-bridged constrained-geometry-type complexes (**4d**). The results can be explained if the presence of a silacyclohexyl bridge increases the stability of the intermediate. It reveals that all of "Cp" ancillary ligand system $(CpCySiN)TiCl_2$ (**4**) showed low catalytic activity under the applied experimental conditions.

CGCs of **5** in combination with $Ph_3CB(C_6F_5)_4/Al(iBu)_3$ were also studied as catalyst precursors for ethylene polymerization (Table 2). A similar trend of activity enhancement observed in **4** was found in the series of **5** as well: a silacyclohexyl bridge (**5d**) (20.9 kgPE mmolTi^{-1}) shows higher activity than that of the silacyclobutyl (**5a**) (6.0 kgPE mmolTi^{-1}) and -pentyl unit (**5c**) (11.3 kgPE mmolTi^{-1}). The "Cp*" ancillary ligand systems show catalytic activities much higher than the "Cp" analogues (**4**). Ethylene polymerization results reveal that modification of the bridgehead by cyclic silylene ring formation has significant effects on catalytic activities when compared with the noncyclic silylene-bridged complex $(Cp^*SiN)TiCl_2$ (9.7 kgPE mmolTi^{-1}).

Given the similar electronic effects among the cyclic silylene groups of **5**, it is reasonable to assume that conformational effects play a key role in alteration of the polymerization activities. It should be noted that the cyclohexyl group in **5d** can have two conformational isomers: a boat form and a chair form. In particular, the chair conformation of the bridge backbone allows two bulky Cp* and *t*Bu groups to adopt ideal positions where the central Ti metal resides in the coordination sphere during the polymerization process. It is noteworthy that the silacyclohexyl ring gives rise to enhanced catalytic activity of the titanium center even though the cyclic ring and titanium center are remote from each other. To obtain information on the effect of the sila-

Table 2. Results of ethylene polymerization.[a]

Entry	Catalyst	Cocatalyst	Temperature [°C]	Activity[b]	$M_w \times 10^{-4}$[c]	M_w/M_n[d]
1	**4a**	$Ph_3CB(C_6F_5)_4$	140	0.22	23.6	2.7
2	**4b**	$Ph_3CB(C_6F_5)_4$	140	0.71	17.8	3.4
3	**4c**	$Ph_3CB(C_6F_5)_4$	140	0.83	28.1	3.1
4	**4d**	$Ph_3CB(C_6F_5)_4$	140	2.45	34.4	3.6
5	**5a**	$Ph_3CB(C_6F_5)_4$	140	6.0	41.8	3.0
6	**5b**	$Ph_3CB(C_6F_5)_4$	140	10.3	39.2	2.8
7	**5c**	$Ph_3CB(C_6F_5)_4$	140	11.3	31.2	2.6
8	**5d**	$Ph_3CB(C_6F_5)_4$	140	20.9	42.7	2.1
9[b]	**5d**	*m*MAO	140	16.4	41.6	7.5
10	$(Cp^*SiN)TiCl_2$	$Ph_3CB(C_6F_5)_4$	140	9.7	40.4	2.9
11	**6d**	$Ph_3CB(C_6F_5)_4$	140	18.6	26.1	2.4
12	$(Cp^*SiN)TiMe_2$	$Ph_3CB(C_6F_5)_4$	140	8.9	24.2	3.3

[a] Polymerization condition: 500-mL autoclave reactor; catalyst = 1 μmol; cocatalyst = trityl borate; scavenger = triisobutylaluminum; [Ti]:[B]:[Al], 1:1.5:100; solvent = heptane (300 mL); ethylene pressure = 30 kg cm^{-2}; time = 10 min. [b] Cocatalyst = *m*MAO; [Ti]:[Al], 1:1500. [c] Kilogram of polymer per mmol of Ti. [d] Weight average molecular weight (g mol^{-1}) and molecular weight distribution measured by PL210 GPC at 135 °C.

cycloalkyl ring, density functional theory (DFT) calculations were performed, and the resulting energy profiles were examined.

Theoretical Consideration of the Structure and Catalytic Activity Relationship

In accordance with the experimental findings, theoretical calculations focused on the influence of the cyclic silylene rings around the metal center. In conjunction with the results from X-ray crystallographic studies, theoretical calculations on each of the conformational isomers derived from the silacycloalkyl ring substitution were carried out. Calculations at the BP86 level of theory revealed that the minimum energy paths for the catalytic reaction steps primarily are confined to the singlet potential energy surface (PES). Table S6 in the Supporting Information summarizes the energy of key stationary points along the reaction paths for **5**. Figure 6 plots the energy profile for the most feasible chain propagation and termination reaction steps. The conformations of the species involved along the reaction paths are also depicted in Figure 6. As for the model system, the "real" cationic alkylmetal(IV) complex is a metal–propylethene complex (Figure 6, center) that is higher in energy than a metal–ethylpropene complex (Figure 6, left) and a metal–pentyl complex (Figure 6, right). An increase in the ring size accelerates the formation of the insertion precursor pentyl complex, whereas termination becomes less favorable, as the energy level of the ethylpropene complex increases. Therefore, more favorable formation of a pentyl complex and less favorable formation of an ethylpropene complex enhance a catalytic activity. DFT calculations corroborate the results of polymerization and show that the propagation step of polymerization is more favorable than the alkyl-transfer step upon increasing the cyclic silylene ring size.

In the case of four-membered silacyclobutyl-bridged complex **5a**, there are two conformational isomers based on DFT calculations, depending on the preference of the Cp* and N*t*Bu groups to be in either the axial or equatorial position of the boat form as shown in Scheme 5. However, it has been noted that there is only a slight difference in energy between two conformers, namely, **5a**-b–a and **5a**-b–e.

On the other hand, six-membered silylene-bridged CGC **5d** has four distinctive conformational isomers arising from both chair and boat conformations with equatorial- and axial-site preference of the Cp* and N*t*Bu groups. (Scheme 4) Figure 6 summarizes the energy profile of each of this species. By taking into account the favorable polymerization

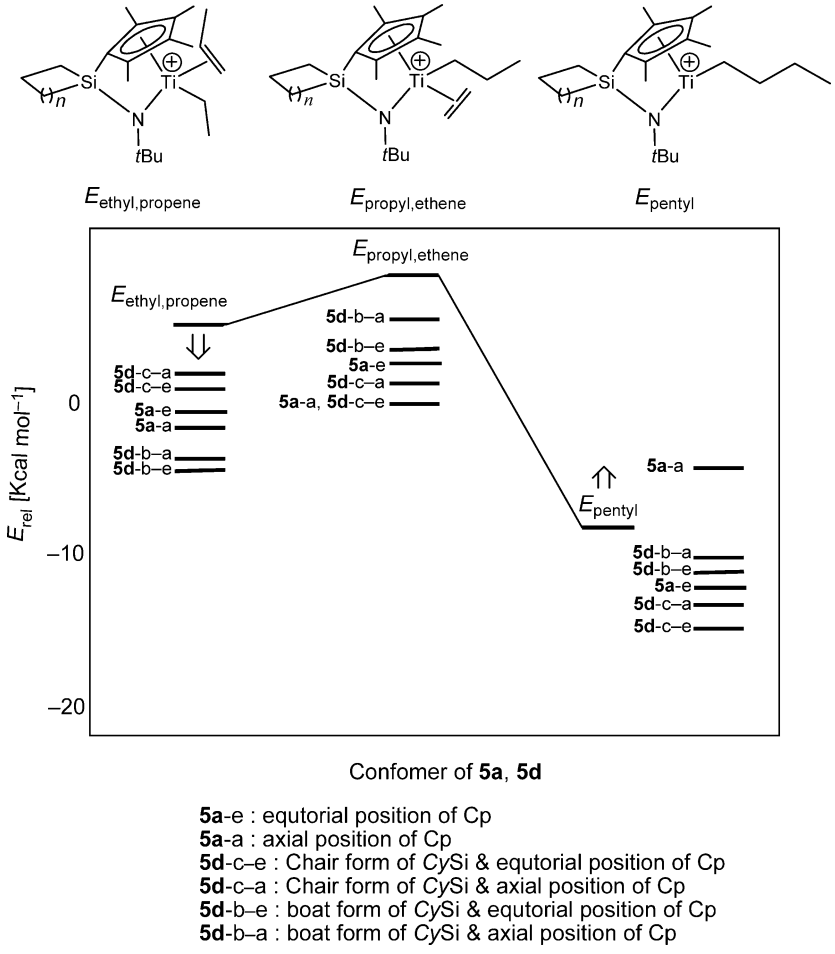

Figure 6. Energy profiles of silacycloalkyl-bridged CGCs **5**.

Table 3. Results of continuous copolymerization of ethylene and 1-octene at elevated temperature.[a]

Catalyst	Cocatalyst	Reaction Temp. [°C]	Catalyst Feed[b]	$M_w \times 10^{-4}$[c]	M_w/M_n[c]	T_m [°C][d]	Density[e]	1-Octene[f] [wt.-%]
6d	$Ph_3CB(C_6F_5)_4$	150	1.5	8.4	2.2	110.7	0.9081	8.8
(Cp*SiN)$TiMe_2$	$Ph_3CB(C_6F_5)_4$	150	3.0	7.8	2.0.	108.2	0.9052	10.8

[a] Continuous polymerization conditions: 400-mL autoclave reactor, solvent = cyclohexane (CHx), TSR (total solution rate) = 5 (kg CHx) h^{-1}, ethylene pressure = 110 kg cm^{-2}, ethylene feed rate = 0.4 kg h^{-1}, 1-octene feed rate = 0.16 kg h^{-1}, scavenger and cocatalyst flow rate wear optimized for each catalyst. [b] μmol (kg CHx)$^{-1}$. [c] Weight average molecular weight (g mol^{-1}) and molecular weight distribution measured by PL210 GPC at 135 °C. [d] T_m measured by DSC. [e] Polymer density measured by a density gradient column based on ASTM D 1505. [f] 1-Octene composition of copolymer calculated from ^{13}C NMR spectrum was measured with a Bruker DRX500 spectrometer (125 MHz) at 120 °C.

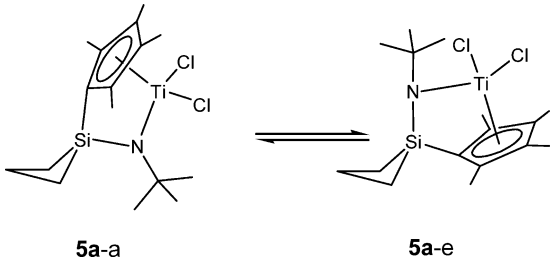

5a-a **5a**-e

Scheme 5. Possible conformational isomers associated with complex **5a**. The second letter "a" and "e" symbolize the position of the Cp* ring in either the axial or equatorial position, respectively.

energy profile having $E_{ethyl,propene} > E_{propyl,ethene} > E_{pentyl}$ in Figure 6, **5d**-c–a and **5d**-c–e are believed to be the better catalyst precursors.

Thus, it can be concluded that conformational isomers derived from the chair form of silacyclohexyl ring **5d** is more stable than the boat form of silacyclobutyl ring **5a**. Conformational isomers associated with **5b** and **5c** are not identified from the calculations as a result of the planar nature of the five-membered silacyclopentenyl and -pentyl rings.

High-Temperature Aging Effect and Enhanced Catalytic Activity on Ethylene and 1-Octene Copolymerization under Continuous Polymerization Process

Compound **5d** was further examined for the use as a high-temperature (up to 200 °C) catalyst and the results are shown in Figure 7. By comparing CGC (Cp*SiN)$TiCl_2$, **5d** exhibited enhanced thermal stability. Even under high-temperature polymerization conditions such as at 200 °C, **5d** is a more efficient catalyst than (Cp*SiN)$TiCl_2$ and produces a high-molecular-weight polymer with narrow molecular weight distribution. Such a promising preliminary result at elevated temperature led us to investigate the characteristics of a silacyclohexyl-bridged CGC catalyst. Dimethylated CGC **6d** was produced in about 58% yield by treating **3** with MeLi (4 equiv.), followed by the addition of $TiCl_4$. Consistent with our previous finding, the dimethylated form of **6d** exhibited catalytic activity higher than that of CGC (Cp*SiN)$TiMe_2$. The molecular weights of polymers produced by **6d** were slightly higher than those of (Cp*SiN)$TiMe_2$ (Table 2, Entry 11 and 12). Regardless of chlorine and methyl ancillary ligands on the precatalyst form, the conformational effect from six-membered silene ring plays an active role in determining the catalytic activity.

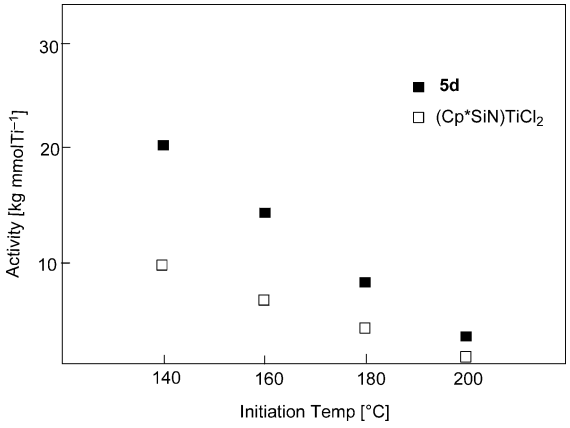

Figure 7. The temperature dependence of activity of **5d** and (Cp*SiN)$TiCl_2$ in the copolymerization of ethylene and 1-octene at elevated temperature.

Finally, copolymerization of ethylene and 1-octene by **6d** was examined by using a continuous polymerization system to avoid a concentration drift. $Ph_3CB(C_6F_5)_4$ and *m*MAO-7 were used as the cocatalyst and scavenger, respectively. Detailed copolymerization results are shown in Table 3.

Conclusions

A series of cyclic silylene-bridged CGC-type metallocenes **4**, **5**, and **6d** were prepared and structurally characterized by utilizing a cyclic silylene ligand backbone as a handle for the enhancement of catalytic performance. Thus, systematic studies on the structures originated from bridging-silylene ring sizes and catalytic activities were carried out to reveal that larger ring size contributes to higher catalytic activities. Thus, silacyclohexyl-modified CGC **5d** exhibited higher catalytic activity both in homo- and copolymerization processes. Among the series investigated, six-membered silacyclohexyl bridged-CGC **5d** showed distinctively discernible conformational isomers, which are believed to be the origin of the higher catalytic activities. Possible isomeric forms associated with the silacyclohexyl backbone were further confirmed by DFT calculations. Detailed investigation regarding the catalytic performance of

6d were carried out under a continuous polymerization process to demonstrate that a silacyclohexyl-modified complex is a superior catalyst system to (Cp*SiN)$TiMe_2$.

Experimental Section

General Procedures: All manipulations were performed under a dry, oxygen-free nitrogen (or argon) atmosphere by using standard Schlenk techniques or in a Vacuum Atmosphere HE-493 dry box. Diethyl ether, toluene, hexane, and pentane were distilled under a nitrogen atmosphere from sodium/benzophenone. Dichloromethane was dried with CaH_2. [D_6]Benzene was distilled under an atmosphere of nitrogen from sodium and stored in a Schlenk storage flask until needed. $CDCl_3$ was predried with CaH_2 and vacuum transferred. *n*BuLi (2.5 M in hexane), MeLi (1.6 M in diethyl ether), and $TiCl_4$ were used as received from Aldrich. Silacycloalkyl chlorides (**1**) were prepared by literature methods.[17] All ^1H (300.1 MHz, measured in $CDCl_3$, C_6D_6) and ^{13}C (75.4 MHz, measured in $CDCl_3$) NMR spectra were recorded with a Varian Mercury-300BB spectrometer unless otherwise stated. ^1H and ^{13}C NMR chemical shifts are reported relative to Me_4Si and were determined by reference to the residual ^1H or ^{13}C solvent peaks. Elemental analyses were performed with a Carlo Erba Instruments CHNS-O EA1108 analyzer. All melting points are uncorrected.

Silacycloalkylcyclopentadienylamide (2)

Step I: Cyclopentadiene (2.39 mL, 30 mmol) in THF (40 mL) was added to a 100-mL flask equipped with a magnetic stirrer and an argon inlet. The solution was cooled to 0 °C and then *n*BuLi (2.5 M in hexanes, 12.0 mL) was added dropwise. The reaction mixture was warmed to room temperature and stirred for an additional 6 h. The resulting solution was cooled to –78 °C again, and then CySiCl_2 (**1**; 5.58 g, 33.0 mmol) was added. The mixture was stirred for 12 h at room temperature, and all volatiles were removed under reduced pressure. The resulting residue was extracted with hexane, filtered through a Celite pad, and dried in vacuo to afford a pale yellow oil.

Step II: CpCySiCl in THF (ca. 40 mL) was added to a 100-mL flask. The solution was cooled to –78 °C and then LiNH*t*Bu (1 equiv.) was added to an additional sidearm over a period of 0.5 h. The reaction was then stirred at room temperature for 2 h, and all volatiles were removed under reduced pressure. The resulting residue was extracted with hexane. The solution was filtered, and the solvent was removed under reduced pressure to leave Cp(cycl)Si(N*t*Bu) as a yellow oil.

2a: Yellow oil (3.99 g, 64.1%). $C_{12}H_{21}NSi$ (207.39): calcd. C 69.50, H 10.21, N 6.75; found C 69.71, H 10.18, N 6.73.

2b: Yellow oil (4.36 g, 66.2%). $C_{13}H_{21}NSi$ (219.40): calcd. C 71.17, H 9.65, N 6.38; found C 70.05, H 9.68, N 6.37

2c: Yellows oil (4.37 g, 65.8%). $C_{13}H_{23}NSi$ (221.41): calcd. C 70.52, H10.47, N 6.33; found C 70.29, H 10.43, N 6.31

2d: Yellow oil (4.71 g, 66.7%). $C_{14}H_{25}NSi$ (235.44): calcd. C 71.42, H 10.70, N 5.95; found C 71.63, H 10.69, N 5.94.

[{η^5:η^1-Cp(cycl)SiN*t*Bu}$TiCl_2$] (4) CGCs: A solution of CpCySi(NH*t*Bu) (**2**; 20.0 mmol) in diethyl ether (80 mL) was cooled to –78 °C. Under a N_2 flush, *n*BuLi (2.5 M in hexanes, 16.0 mL) was added dropwise to a solution of **2**. The reaction mixture was stirred overnight and all volatiles were removed under reduced pressure. The product residue was washed once with hexane (50 mL) and then dried under vacuum to afford Li_2[CpCySi(N*t*Bu)] as a white powder. To a precooled solution at –78 °C containing Li_2[Cp(cycl)Si(N*t*Bu)] (10.0 mmol) was added $TiCl_4$ (1.0 M in toluene, 9.5 mL) diluted in a toluene (ca. 50 mL). The solution was stirred at room temperature for 6 h. All volatiles were removed under reduced pressure. Extraction with hexane, followed by the filtration and evaporation of the solvent, gave red crude products. Further purification by recrystallization at –35 °C from hexane gave yellow crystals of **4**.

4a: Yellow crystals (0.64 g, 19.7%). $C_{12}H_{19}Cl_2NSiTi$ (324.14): calcd. C 44.46, H 5.91, N 4.32; found C 44.53, H 5.90, N 4.34.

4b: Yellow crystals (0.69 g, 20.4%). $C_{13}H_{19}Cl_2NSiTi$ (336.16): calcd. C 46.45, H 5.70, N 4.17; found C 46.39, H 5.70, N 4.17.

4c: Yellow crystals (0.68 g, 20.1%). $C_{13}H_{21}Cl_2NSiTi$ (338.17): calcd. C 46.17, H 6.26, N 4.14; found C 46.55, H 6.13, N 4.16.

4d: Yellow crystals (0.74 g, 20.9%). $C_{14}H_{23}Cl_2NSiTi$ (352.20): calcd. C 47.74, H 6.58, N 3.98; found C 47.46, H 6.37, N 3.88.

Silacycloalkyl-1,2,3,4-tetramethylcyclopentadienylamide (3): A procedure similar to that used for **2** was implemented, but starting from tetramethylcyclopentadiene (30 mmol).

3a: Yellow oil (6.56 g, 83%). $C_{16}H_{29}NSi$ (263.49): calcd. C 72.93, H 11.09, N 5.32; found C 72.85, H 11.12, N 5.33.

3b: Yellow oil (7.42 g, 85%). $C_{17}H_{29}NSi$ (275.50): calcd. C 74.11, H 10.61, N 5.08; found C 73.84, H 10.62, N 5.09.

3c: Yellow oil (6.99 g, 84%). $C_{17}H_{31}NSi$ (277.52): calcd. C 73.57, H 11.26, N 5.05; found C 73.86, H 11.30, N 5.06.

3d: Yellow oil (7.02 g, 85%). $C_{18}H_{33}NSi$ (291.55): calcd. C 74.15, H 11.41, N 4.80; found C 74.10, H 11.39, N 4.82.

[{η^5:η^1-(C_5Me_4)Cp(cycl)SiN*t*Bu}$TiCl_2$] (5) CGCs: A procedure similar to that used for **4** was implemented, but starting from Cp*CySi(NH*t*Bu) (**3**; 20 mmol). At the final step of purification, pentane was used as the recrystallization solvent. Low-temperature recrystallization at –35 °C produced yellow crystals.

5a: Yellow crystals (0.40 g, 10.4%). $C_{16}H_{27}Cl_2NSiTi$ (380.25): calcd. C 50.54, H 7.16, N 3.68; found C 50.93, H 7.06, N 3.72.

5b: Yellow crystals (0.49 g, 12.5%). $C_{17}H_{27}Cl_2NSiTi$ (392.26): calcd. C 52.05, H 6.94, N 3.57; found C 51.64, H 6.84, N 3.51.

5c: Yellow crystals (0.45 g, 11.3%). $C_{17}H_{29}Cl_2NSiTi$ (394.28): calcd. C 51.79, H 7.41, N 3.55; found C 52.19, H 7.30, N 3.59.

5d: Yellow crystals (0.52 g, 12.7%). $C_{18}H_{31}Cl_2NSiTi$ (408.30): calcd. C 52.95, H 7.65, N 3.43; found C 52.64, H 7.41, N 3.35.

[{η^5:η^1-(C_5Me_4)Cp(cycl)SiN*t*Bu}$TiMe_2$] (6d) CGC: MeLi (1.6 M in diethyl ether, 19.41 mL, 31.03 mmol) was added dropwise at –78 °C to a solution of [(C_5Me_4)Cp(cycl)Si(NH*t*Bu)] (2.24 g, 7.68 mmol) in diethyl ether. The white suspension was stirred for 2 h at room temperature. Then, $TiCl_4$ (0.83 mL, 7.68 mmol) in hexane (20 mL) was slowly added at room temperature to the lithium salt, and the resulting black mixture was stirred for 6 h. The solvent was removed under reduced pressure to give a black solid, which was extracted with hexane. A yellow microcrystalline powder (1.53 g, 57.9%) of **6d** was obtained by recrystallization from pentane at –35 °C. $C_{20}H_{37}NSiTi$ (367.47): calcd. C 65.37, H 10.15, N 3.81; found C 64.73, H 10.04, N 3.73.

Ethylene Polymerization: Heptane (300 mL) and TIBA [triisobutylaluminum, Al(*i*Bu)$_3$] were introduced to a thoroughly dried 500-mL autoclave reactor, and the reactor was heated up to 140 °C. The reactor was pressurized with ethylene up to 30 kg cm^{-2} and specific amounts of catalyst and $Ph_3CB(C_6F_5)_4$ toluene solution

were added through a catalyst injector to start polymerization. During polymerization, the reactor pressure was maintained constant by continuously feeding ethylene. After 10 min, the reactor was cooled down to 55 °C, degassed, and acidic ethanol (5 mL) was added to stop polymerization. The solution was then poured into ethanol (1500 mL), and the resultant polymer was recovered by filtration and dried in vacuo at 70 °C for 12 h.

Continuous Copolymerization of Ethylene and 1-Octene: A 400-mL CSTR (continuous stirred tank reactor) was used for copolymerization. Catalyst, cocatalyst, scavenger, cyclohexane, ethylene, and 1-octene were added continuously by using metering pumps, and recovery of unreacted monomer and solvent was also performed continuously. The CSTR was maintained at 150 °C and 110 kg cm^{-2} and all process variables including feed rates were computer-controlled by using FIX software. To product solution coming out of the CSTR was added pelagonic acid at a flow rate of 5.2 mmol h^{-1} to deactivate the catalyst residues. Then, unreacted monomers and solvent were removed from the polymer solution, and the polymeric product was recovered. Figure 8 shows the plot of $Q/(1 - Q)\tau$ vs. catalyst concentration [μmol kg^{-1}], where Q and τ are ethylene conversion and reactor hold-up time, respectively. The rate of disappearance of ethylene is given by $-d[E]/dt = k_p[Cat^*][E]$, where $[E]$ = ethylene concentration, $[Cat^*]$ = active catalyst concentration, and k_p = reaction rate constant. The CSTR system[18] is given by $-d[E]/dt = V_{fl.}[E]_{in}Q/V_r$, where $V_{fl.}$ = volume of fluid, Q = ethylene conversion, $[E]_{in}$ = inlet ethylene concentration, $[E]_{out}$ = outlet ethylene concentration, V_r = volume of reactor. By combining the two equations, $k_p[Cat^*]V_{fl.}/V_r = Q/(1 - Q)$ is derived. Because $V_{fl.}/V_r$ is the reactor hold-up time (τ), this equation becomes $k_p[Cat^*] = Q/[\tau(1 - Q)]$. If $Q/[\tau(1 - Q)]$ is plotted against $[Cat^*]$, a straight line is obtained with a slope of k_p, as shown in Figure 8.

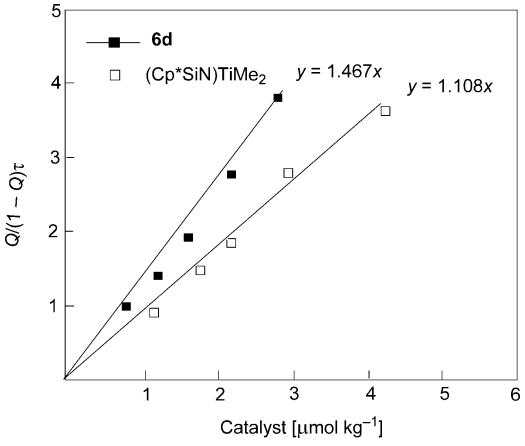

Figure 8. Catalyst activity for **6d** and $(Cp^*SiN)TiMe_2$ in continuous copolymerization of ethylene and 1-octene at elevated temperature (see Table 3), $Q/(1 - Q)\tau$ vs. catalyst concentration; Q: ethylene conversion, τ: reactor hold-up time.

Crystal Structure Determination: Crystals of **4b**, **4c**, **5a**, **5b**, and **5d** were obtained from either hexane or pentane solutions at –35 °C, sealed in glass capillaries under an atmosphere of argon, and mounted on the diffractometer. Preliminary examination and data collection for **4b** and **4c** were performed with an Enraf CAD4 automated diffractometer equipped with a sealed-tube X-ray source (50 kV × 30 mA) by using graphite-monochromated Mo-K_α radiation (λ = 0.71073 Å). The unit cell was determined by using search, center, index, and least-squares routines. The intensity data were corrected for Lorentz and polarization effects and for anisotropic decay. Empirical absorption corrections based on ψ scans were also applied.

Preliminary examination and data collection for **5a**, **5c**, and **5d** were performed by using a Bruker SMART CCD detector system single-crystal X-ray diffractometer equipped with a sealed-tube X-ray source (50 kV × 30 mA) by using graphite-monochromated Mo-K_α radiation (λ = 0.71073 Å). Preliminary unit cell constants were determined with a set of 45 narrow-frame (0.3° in ω) scans. The double-pass method of scanning was used to exclude any noise. The collected frames were integrated by using an orientation matrix determined from the narrow-frame scans. The SMART software package was used for data collection, and SAINT was used for frame integration.[19a] Final cell constants were determined by a global refinement of *xyz* centroids of reflections harvested from the entire data set. Structure solution and refinement were carried out by using the SHELXTL-PLUS software package.[19b] The absolute configuration of **5d** was confirmed by the refinement of the Flack parameter. CCDC-658193, -658194, -658195, -658196, and -658197 contain the supplementary crystallographic data for this paper. These data can be obtained free of charge from The Cambridge Crystallographic Data Centre via www.ccdc.cam.ac.uk/data_request/cif.

Computational Details: Stationary points on the potential energy surface were calculated by using the Amsterdam density functional (ADF) program, developed by Baerends et al.[20a,20b] and vectorized by Ravenek.[20c] The numerical integration scheme applied for the calculations was developed by te Velde et al.[20d,20e] The geometry optimization procedure was based on the method similar to that of Versluis and Ziegler.[20f] The electronic configurations of the molecular systems were described by double-ζ STO basis sets with polarization functions for the H, N and C atoms, whereas triple-ζ Slater-type basis sets were employed for the Si and Ti atoms.[20g,20h] The 1s electrons of N and C, and the 1s-2p electrons of Si and Ti were treated as frozen cores. A set of auxiliary[20i] s, p, d, f, and g STO functions, centered on all nuclei, was used in order to fit the molecular density and the Coulomb and exchange potentials in each SCF cycle. Energy differences were calculated by augmenting the local exchange-correlation potential through Vosko et al.[20j] with Becke's[20k] nonlocal exchange corrections and Perdew's[20l,20m] nonlocal correlation corrections (BP86). Geometries were optimized by including nonlocal corrections at this level of theory. ZORA scalar relativistic corrections[20n,20o] were added variationally to the total energy for all systems. In view of the fact that each system investigated in this work shows a large HOMO–LUMO gap, a spin-restricted formalism was used for all calculations. No symmetry constraints were used.

Supporting Information (see footnote on the first page of this article): Characterization data for **2**–**5**; crystal data and structure refinement data for **4b**, **4c**, **5a**, **5c**, **5d**; molecular structures of **4b**, **4c**; energies of *Cy*Si(N*t*Bu)(C_5Me_4)Ti(C_2H_5)(propene) and *Cy*Si(N*t*Bu) (C_5Me_4)TiC_5H_{11} relative to *Cy*Si(N*t*Bu)(C_5Me_4)Ti(C_3H_7)(ethene); optimized geometries of selected structures.

Acknowledgments

This work was supported by the Korea Research Foundation Grant funded by the Korean Government MOEHRD (KRF-2005-070-C00072).

[1] a) E. E. Bunel, B. J. Burger, J. E. Bercaw, *J. Am. Chem. Soc.* **1988**, *110*, 976–978; b) W. E. Piers, P. J. Shapiro, E. E. Bunel, J. E. Bercaw, *Synlett* **1990**, *2*, 74–84; c) P. J. Shapiro, E. E. Bunel, P. J. Schaefer, J. E. Bercaw, *Organometallics* **1990**, *9*, 867–869; d) P. J. Shapiro, W. D. Cotter, W. P. Schaefer, J. A. Labinger, J. E. Bercaw, *J. Am. Chem. Soc.* **1994**, *116*, 4623–4640.

[2] a) J. Okuda, F. J. Schattenmann, S. Wokadlo, W. Massa, *Organometallics* **1995**, *14*, 789–795; b) K. E. Du plooy, U. Moll, S. Wokadlo, W. Massa, J. Okuda, *Organometallics* **1995**, *14*, 3129–3131.

[3] a) A. L. McKnight, R. M. Waymouth, *Chem. Rev.* **1998**, *98*, 2587–2598; b) A. L. McKnight, M. A. Masood, R. M. Waymouth, D. A. Straus, *Organometallics* **1997**, *16*, 2879–2885; c) J. Okuda, T. Eberle "Half-Sandwich Complexes as Metallocene Analogues" in *Metallocenes – Synthesis, Reactivity, Applications* (Eds.: A. Togni, R. L. Haltermann), Wiley-VCH, Weinheim, **1998**, vol. 1, pp. 415–453.

[4] a) A. K. Hughes, A. Meetsma, J. H. Teuben, *Organometallics* **1993**, *12*, 1936–1945; b) D. D. Devore, F. J. Timmers, D. L. Hasha, R. K. Rosen, T. J. Marks, P. A. Deck, C. L. Stern, *Organometallics* **1995**, *14*, 3132–3134; c) S. Ciruelos, T. Cuenca, R. Gómez, P. Gómez-Sal, A. Manzanero, P. Royo, *Organometallics* **1996**, *15*, 5577–5585; d) Y. Liang, G. P. A. Yap, A. L. Rheingold, K. H. Theopold, *Organometallics* **1996**, *15*, 5284–5286; e) P.-J. Sinnema, L. van der Veen, A. L. Speck, N. Veldman, J. H. Teuben, *Organometallics* **1997**, *16*, 4245–4247; f) P. T. Witte, A. Meetsma, B. Hessen, P. H. M. Budzelaar, *J. Am. Chem. Soc.* **1997**, *119*, 10561–10562; g) P. T. Gomes, M. L. H. Green, A. M. Martins, *J. Organomet. Chem.* **1998**, *551*, 133–138; h) L. Schwink, P. Knochel, T. Eberle, J. Okuda, *Organometallics* **1998**, *17*, 7–9; i) S. J. Brown, X. Gao, D. G. Harrison, L. Koch, R. E. v. H. Spence, G. P. A. Yap, *Organometallics* **1998**, *17*, 5445–5447; j) S. Feng, J. Klosin, J. K. William Jr, M. H. McAdon, D. R. Neithamer, P. N. Nickias, J. T. Patton, D. R. Wilson, K. A. Abboud, C. L. Stern, *Organometallics* **1999**, *18*, 1159–1167; k) A. J. Ashe III, X. Fang, J. W. Kampf, *Organometallics* **1999**, *18*, 1363–1365; l) D. van Leusen, D. J. Beetstra, B. Hessen, J. H. Teuben, *Organometallics* **2000**, *19*, 4084–4089; m) H. Braunschweig, C. von Koblinski, U. Englert, *Chem. Commun.* **2000**, *12*, 1049–1050; n) H. Juvaste, T. T. Pakkanen, E. I. Iiskola, *Organometallics* **2000**, *19*, 1729–1733; o) S. Gentil, N. Pirio, P. Meunier, J. C. Gallucci, J. D. Schloss, L. A. Paquette, *Organometallics* **2000**, *19*, 4169–4172; p) H. G. Alt, A. Reb, W. Milius, A. Weis, *J. Organomet. Chem.* **2001**, *628*, 169–182; q) A. Novak, A. J. Blake, C. Wilson, J. B. Love, *Chem. Commun.* **2002**, *23*, 2796–2797; r) K. Kunz, G. Erker, S. Döring, R. Fröhlich, G. Kehr, *J. Am. Chem. Soc.* **2001**, *123*, 6181.

[5] a) H. V. R. Diaz, Z. Wang, S. G. Bott, *J. Organomet. Chem.* **1996**, *508*, 91–99; b) M. Enders, R. Rudolph, H. Pritzkow, *J. Organomet. Chem.* **1997**, *549*, 251–256; c) B. Rieger, *J. Organomet. Chem.* **1991**, *420*, C17–C20; d) S. D. R. Christie, K. W. Man, R. J. Whitby, A. M. Z. Slawin, *Organometallics* **1999**, *18*, 348–359; e) Bertuleit, A. M. Könemann, L. Duda, G. Erker, R. Fröhlich, *Top. Catal.* **1999**, *7*, 37–44; f) K. Thorshaug, R. Mendichi, L. Boggioni, I. Tritto, S. Trinkle, C. Friedrich, R. Mühaupt, *Macromolecules* **2002**, *35*, 2903–2911; g) G. Altenhoff, S. Bredeau, G. Erker, G. Kehr, O. Kataeva, R. Fröhlich, *Organometallics* **2002**, *21*, 4084–4089; h) K. Kunz, G. Erker, S. Döring, S. Bredeau, G. Kher, R. Fröhlich, *Organometallics* **2002**, *21*, 1031–1041; i) L. Li, M. V. Metz, H. Li, M.-C. Chen, T. J. Marks, L. Liable-Sands, A. L. Rheingold, *J. Am. Chem. Soc.* **2002**, *124*, 12725–12741; j) N. Naga, A. Toyota, K. Ogino, *J. Polym. Sci., Part A Polym. Chem* **2005**, *43*, 911–915; k) N. Naga, *J. Polym. Sci., Part A Polym. Chem* **2005**, *43*, 1285–1291; l) S. Martínez, M. T. Exposito, J. Ramos, V. Cruz, M. C. Martínez, M. López, A. Muñoz-Escalona, J. Martínez-Salazar, *J. Polym. Sci., Part A Polym. Chem.* **2005**, *43*, 711–725; m) A. R. Lavoie, R. M. Waymouth, *Tetrahedron* **2004**, *60*, 7147–7155; n) A. Eisenhardt, W. Kaminsky, *Catal. Commun.* **2004**, *5*, 653–657; o) F. Song, R. D. Cannon, S. J. Lancaster, M. Bochmann, *J. Mol. Caltal. A Chem* **2004**, *218*, 21–28; p) K. Musikabhumma, T. P. Spaniol, J. Okuda, *J. Mol. Caltal. A Chem* **2004**, *218*, 73–81; q) M. Sudupe, J. Cano, P. Royo, E. Herdtweck, *Eur. J. Inorg. Chem.* **2004**, 3074–3083.

[6] a) J. Klosin, J. K. William Jr, P. N. Nickias, G. R. Roof, P. De Waele, K. A. Abboud, *Organometallics* **2001**, *20*, 2663–2665; b) G. Jimenez, P. Royo, T. Cuenca, E. Herdtweck, *Organometallics* **2002**, *21*, 2189–2195; c) V. V. Kotov, E. V. Avtomonov, J. Sundermeyer, K. Harms, D. A. Lemenovskii, *Eur. J. Inorg. Chem.* **2002**, 678–691; d) H. G. Alt, A. Weis, A. Reb, R. Ernst, *Inorg. Chim. Acta* **2003**, *343*, 253–274; e) R. M. Kasi, E. B. Coughlin, *Organometallics* **2003**, *22*, 1534–1539; f) C. De Rosa, F. Auriemma, O. Ruiz de Ballesteros, L. Resconi, A. Fait, E. Ciaccia, I. Camurati, *J. Am. Chem. Soc.* **2003**, *125*, 10913–10920; g) T. R. Boussie, G. M. Diamond, C. Goh, K. A. Hall, A. M. LaPointe, M. Leclerc, C. Lund, V. Murphy, J. A. W. Shoemaker, U. Tracht, H. Turner, J. Zhang, T. Uno, R. K. Rosen, J. C. Stevens, *J. Am. Chem. Soc.* **2003**, *125*, 4306–4317; h) M. W. McKittrick, C. W. Jones, *J. Am. Chem. Soc.* **2004**, *126*, 3052–3053; i) H. Braunschweig, F. M. Breitling, C. von Koblinski, A. J. P. White, D. J. Williams, *Dalton Trans.* **2004**, *6*, 938–943; j) L. J. Irwin, J. H. Reibenspies, S. A. Miller, *J. Am. Chem. Soc.* **2004**, *126*, 16716–16717; k) H. Li, L. Li, D. J. Schwartz, M. V. Metz, T. J. Marks, L. Liable-Sands, A. L. Rheingold, *J. Am. Chem. Soc.* **2005**, *127*, 14756–14768; l) J. Cano, M. Sudupe, P. Royo, M. E. G. Mospuera, *Organometallics* **2005**, *24*, 2424–2432; m) D. J. Joe, C. J. Wu, T. Bok, E. J. Lee, C. H. Lee, W.-S. Han, S. O. Kang, B. Y. Lee, *Dalton Trans.* **2006**, 4056–4062; n) G. Erker, *Coord. Chem. Rev.* **2006**, *250*, 1056; o) J. Cano, M. Sudupe, P. Royo, M. E. G. Mosquera, *Angew. Chem. Int. Ed.* **2006**, *45*, 7572–7574; p) S. Bambirra, D. V. Leusen, C. G. J. Tazelaar, A. Meetsma, B. Hessen, *Organometallics* **2007**, *26*, 1014–1023.

[7] a) J.-F. Carpentier, V. P. Maryin, J. Luci, R. F. Jordan, *J. Am. Chem. Soc.* **2001**, *123*, 898–909; b) E. Kirillov, L. Toupet, C. W. Lehmann, A. Razavi, J.-F. Capentier, *Organometallics* **2003**, *22*, 4467–4479; c) J. Okuda, *Dalton Trans.* **2003**, 2367–2378; d) S. Bredeau, G. Altenhoff, K. Kunz, S. Döring, S. Grimme, G. Kehr, G. Erker, *Organometallics* **2004**, *23*, 1836–1844; e) J. Wang, H. Li, N. Guo, L. Li, C. L. Stern, T. J. Marks, *Organometallics* **2004**, *23*, 5112–5114; f) A. R. Lavoie, R. M. Waymouth, *Tetrahedron* **2004**, *60*, 7147–7155; g) A. N. Ryabov, A. Z. Voskoboynikov, *J. Organomet. Chem.* **2005**, *690*, 4213–4221; h) K. A. O. Starzewski, B. S. Xin, N. Steinhauser, J. Schweer, J. Benet-Buchholz, *Angew. Chem. Int. Ed.* **2006**, *45*, 1799–1803; i) K. Nishii, H. Hagihara, T. Ikeda, M. Akita, T. Shiono, *J. Organomet. Chem.* **2006**, *691*, 193–201; j) A. Bartol-Scott, H. Braunschweig, T. Kupfer, M. Lutz, I. Manner, T.-L. Nguyen, K. Radacki, F. Seeler, *Chem. Eur. J.* **2006**, *12*, 1266–1273; k) R. G. Howe, C. S. Tredget, S. C. Lawrence, S. Subongkoj, A. R. Cowley, P. Mountford, *Chem. Commun.* **2006**, 223–225; l) C. Ramos, P. Royo, M. Lanfranchi, M. A. Pellinghelli, A. Tiripicchio, *Organometallics* **2007**, *26*, 445–454.

[8] a) B. Wang, B. Mu, X. Deng, H. Cui, S. Xu, X. Zhou, F. Zou, Y. Li, L. Yang, Y. Li, Y. Hu, *Chem. Eur. J.* **2005**, *11*, 669–679; b) S. Gómez-Ruiz, S. Prashar, M. Fajardo, A. Antiñolo, A. Otero, M. A. Maestro, V. Volkis, M. S. Eisen, C. J. Pastor, *Polyhedron* **2005**, *24*, 1298–1313; c) A. Antiñolo, M. Fajardo, S. Gómez-Ruiz, I. López-Solera, A. Otero, S. Prashar, A. M. Rodríguez, *J. Organomet. Chem.* **2003**, *683*, 11–22.

[9] a) S.-J. Kim, I. N. Jung, B. R. Yoo, S. Cho, J. Ko, S. H. Kim, S. O. Kang, *Organometallics* **2001**, *20*, 1501–1503; b) S.-J. Kim, D.-W. Choi, Y.-J. Lee, B.-H. Chae, J. Ko, S. O. Kang, *Organometallics* **2004**, *23*, 559–567; c) T. W. Woo, M. A. Ok, J. S. Hahn, S. O. Kang, J. H. Jung, PCT Int. Appl. WO 07–29986, 2007.

[10] a) J. C. Stevens, F, J. Timmers, D. R. Wilson, G. F. Schmidt, P. N. Nickias, R. K. Rosen, G. W. Knight, S. Lai (Dow Chemical Co.), EP 416815–A2, **1991** ; b) J. M. Canich (Exxon Chemi-

cal Co.), EP 420436–A1, **1991**; WO 92–00333, **1992**; c) G. W. Knight, R. A. Maugans, E. N. Knickerbocker, WO 94–25647, **1994**; d) K. W. McKay, R. R. Banchard, E. R. Feig, K. G. Kummer, WO. 94–06865, **1994**.

[11] C. Wang, G. Erker, G. Kehr, K. Wedeking, R. Fröhlich, *Organometallics* **2005**, *24*, 4760–4773.

[12] S.-J. Kim, Y. J. Lee, E. Kang, S. H. Kim, B. Lee, M. Cheong, I.-H. Suh, S. O. Kang, *Organometallics* **2003**, *22*, 3958–3966.

[13] S.-J. Kim, I. N. Jung, B. R. Yoo, S. H. Kim, J. Ko, D. Byun, S. O. Kang, *Organometallics* **2001**, *20*, 2136–2144.

[14] a) L. Resconi, I. Camurati, C. Grandini, M. Rinaldi, N. Mascellani, O. Traverso, *J. Organomet. Chem.* **2002**, *664*, 5–26; b) C. Grandini, I. Camurati, S. Guidotti, N. Mascellani, L. Resconi, *Organometallics* **2004**, *23*, 344.

[15] D. W. Carpenetti, L. Kloppenburg, J. T. Kupec, J. L. Petersen, *Organometallics* **1996**, *15*, 1572–1581.

[16] a) K. E. du Plooy, U. Rose, H.-C. Kang, J. Okuda, W. Massa, *Chem. Ber.* **1996**, *129*, 275; b) Y.-X. Chen, C. L. Stern, S. Yang, T. J. Marks, *J. Am. Chem. Soc.* **1996**, *118*, 12451; c) T. K. Woo, P. M. Margl, J. C. W. Lohrenz, P. E. Blochl, T. Ziegler, *J. Am. Chem. Soc.* **1996**, *118*, 13021; d) W. A. Herrmann, M. J. A. Morawietz, *J. Organomet. Chem.* **1994**, *482*, 169; e) L. Kloppenburg, J. L. Petersen, *Organometallics* **1996**, *15*, 7; f) Y.-X. Chen, T. J. Marks, *Organometallics* **1997**, *16*, 3649; g) F. Amor, T. P. Spaniol, J. Okuda, *Organometallics* **1997**, *16*, 4765; h) L. Duda, G. Erker, R. Fröhlich, F. Zipple, *Eur. J. Inorg. Chem.* **1998**, 1153; i) T. Eberle, T. P. Spaniol, J. Okuda, *Eur. J. Inorg. Chem.* **1998**, 237; j) M. Könemann, G. Erker, R. Fröhlich, E.-U. Würthwein, *J. Am. Chem. Soc.* **1997**, *119*, 11155; k) B. Rieger, *J. Organomet. Chem.* **1991**, *420*, C17; l) I. M. Ewen, P. Ahlberg, *J. Am. Chem. Soc.* **1992**, *114*, 10869; m) H. V. R. Dias, Z. Wang, S. G. Bott, *J. Organomet. Chem.* **1996**, *508*, 91; n) H. V. R. Dias, Z. Wang, *J. Organomet. Chem.* **1997**, *539*, 77; o) J. Okuda, *Chem. Ber.* **1990**, *123*, 1649; p) F. Amor, J. Okuda, *J. Organomet. Chem.* **1996**, *520*, 245; q) J. Okuda, S. Verch, T. P. Spaniol, R. Stürmer, *Chem. Ber.* **1996**, *129*, 1429; r) J. Okuda, T. Eberle, T. P. Spaniol, *Chem. Ber.* **1997**, *130*, 209; s) G. Xu, E. Ruckenstein, *Macromolecules* **1998**, *31*, 4724; t) W.-J. Wang, D. Yan, S. Zhu, A. E. Hamielec, *Macromolecules* **1998**, *31*, 8677; u) M. Galan-Fereres, T. Koch, E. Hey-Hawkins, M. S. Eisen, *J. Organomet. Chem.* **1999**, *580*, 145; v) A. L. Mcknight, R. M. Waymouth, *Macromolecules* **1999**, *32*, 2816; w) P. S. Chum, W. J. Kuper, M. J. Guest, *Adv. Mater.* **2000**, *12*, 1759; x) W.-J. Wang, S. Zhu, *Macromolecules* **2000**, *33*, 1157; y) W.-J. Wang, S. Zhu, S.-J. Park, *Macromolecules* **2000**, *33*, 5770; z) H. G. Alt, A. Reb, K. Kundu, *J. Organomet. Chem.* **2001**, *628*, 211.

[17] a) R. West, *J. Am. Chem. Soc.* **1954**, *76*, 6012–6014; b) J. Laane, *J. Am. Chem. Soc.* **1967**, *89*, 1144–1147; c) R. Damrauer, A. Simon, M. G. Laporterie, Y. T. Park, W. P. Weber, *J. Organomet. Chem.* **1990**, *391*, 7–12.

[18] O. Levenspiel, *Chemical Reaction Engineering*, 2nd ed., Tower press, **1985**, pp. 101–103.

[19] a) G. M. Sheldrick, *Acta Crystallogr.* **1990**, *A46*, 467; b) G. M. Sheldrick, *SHELXL: Program for Crystal Structure Refinement*, University of Göttingen, Germany, **1997**.

[20] a) E. J. Baerends, D. E. Ellis, P. Ros, *Chem. Phys.* **1973**, *2*, 41; b) E. J. Baerends, P. Ros, *Chem. Phys.* **1973**, *2*, 52; c) W. Ravenek in *Algorithms and Applications on Vector and Parallel Computers* (Eds.: H. J. J. te Riele, T. J. Dekker, H. A. van de Horst), Elsevier, Amsterdam, **1987**; d) G. te Velde, E. J. J. Baerends, *Comput. Chem.* **1992**, *99*, 84; e) P. M. Boerrigter, G. te Velde, E. J. Baerends, *Int. J. Quantum Chem.* **1988**, *33*, 87; f) L. Versluis, T. Ziegler, *J. Chem. Phys.* **1988**, *88*, 322; g) J. G. Snijders, E. J. Baerends, P. Vernoijs, *At. Nucl. Data Tables* **1982**, *26*, 483; h) P. Vernoijis, J. G. Snijders, E. J. Baerends, *Slater Type Basis Functions for the Whole Periodic System*; Internal Report (in Dutch), Department of Theoretical Chemistry, Free University, Amsterdam, **1981**; i) J. Krijn, E. J. Baerends, *Fit Functions in the HFS Method*, Internal Report (in Dutch), Department of Theoretical Chemistry, Free University, Amsterdam, **1984**; j) S. H. Vosko, L. Wilk, M. Nusair, *Can. J. Phys.* **1980**, *58*, 1200; k) A. Becke, *Phys. Rev. A* **1988**, *38*, 3098; l) J. P. Perdew, *Phys. Rev. B* **1986**, *34*, 7406; m) J. P. Perdew, *Phys. Rev. B* **1986**, *33*, 8822; n) E. van Lenthe, A. E. Ehlers, E. J. Baerends, *J. Chem. Phys.* **1999**, *110*, 8943; o) E. van Lenthe, E. J. Baerends, J. G. Snijders, *J. Chem. Phys.* **1993**, *99*, 4597.

Received: December 5, 2007
Published Online: March 19, 2008

